Biochemical and Biophysical Research Communications 455 (2014) 290–297

Contents lists available at ScienceDirect

Biochemical and Biophysical Research Communications

journal homepage: www.elsevier.com/locate/ybbrc

A mutation in the mitochondrial protein UQCRB promotes angiogenesis through the generation of mitochondrial reactive oxygen species

Junghwa Chang [a], Hye Jin Jung [b], Seung Hun Jeong [d], Hyoung Kyu Kim [d], Jin Han [d], Ho Jeong Kwon [a,c,*]

[a] Chemical Genomics National Research Lab., Department of Biotechnology, Translational Research Center for Protein Function Control, College of Life Science & Biotechnology, Yonsei University, Seoul 120-749, Republic of Korea
[b] Department of Pharmaceutical Engineering, Sun Moon University, Asansi, Chungnam 330-150, Republic of Korea
[c] Department of Internal Medicine, Yonsei University College of Medicine, Seoul 120-752, Republic of Korea
[d] National Research Laboratory for Mitochondrial Signaling, Department of Physiology, College of Medicine, Department of Health Sciences and Technology, Cardiovascular and Metabolic Disease Center, Inje University, Busan, Republic of Korea

ARTICLE INFO

Article history:
Received 27 October 2014
Available online 11 November 2014

Keywords:
Angiogenesis
Complex III
Mitochondria
Mitochondrial reactive oxygen species
UQCRB

ABSTRACT

Ubiquinol-cytochrome c reductase binding protein (UQCRB) is one of the subunits of mitochondrial complex III and is a target protein of the natural anti-angiogenic small molecule terpestacin. Previously, the biological role of UQCRB was thought to be limited to the maintenance of complex III. However, the identification and validation of UQCRB as a target protein of terpestacin enabled the role of UQCRB in oxygen sensing and angiogenesis to be elucidated. To explore the biological role of this protein further, UQCRB mutant stable cell lines were generated on the basis of a human case report. We demonstrated that these cell lines exhibited glycolytic and pro-angiogenic activities via mitochondrial reactive oxygen species (mROS)-mediated HIF1 signal transduction. Furthermore, a morphological abnormality in mitochondria was detected in UQCRB mutant stable cell lines. In addition, the proliferative effect of the UQCRB mutants was significantly regulated by the UQCRB inhibitors terpestacin and A1938. Collectively, these results provide a molecular basis for UQCRB-related biological processes and reveal potential key roles of UQCRB in angiogenesis and mitochondria-mediated metabolic disorders.

1. Introduction

The electron transport chain (ETC) of mitochondria consists of five complexes and plays a crucial role in energy production by ATP synthesis [1]. Numerous reports have indicated the involvement of various mitochondrial proteins in multiple diseases such as metabolic diseases and cancers [1–4]. However, information on the relationship between complex III and angiogenesis is limited.

Ubiquinol-cytochrome c reductase binding protein (UQCRB), a nuclear-encoded 13.4-kDa subunit of complex III, has been shown to play a role in the electron transport and maintenance of complex III [5]. Recently, a potential role of UQCRB in angiogenesis has been demonstrated by identifying it as a target of the natural anti-angiogenesis inhibitor terpestacin [6]. UQCRB is involved in mitochondrial reactive oxygen species (mROS)- and hypoxia-inducible factor (HIF)-mediated angiogenesis by modulating the oxygen-sensing mechanism that regulates hypoxia responses. Moreover, UQCRB regulates vascular endothelial growth factor receptor 2 (VEGFR2)-signaling-induced angiogenesis [7]. In addition, recent studies have demonstrated that various genetic variations of UQCRB were observed in several cancers, including hepatocellular carcinoma [8], ovarian cancer [9], pancreatic ductal adenocarcinoma [10], and colorectal cancer [11]. This potential of UQCRB to causes disease indicates its important role in angiogenesis and other mitochondria-mediated disorders.

In a recent report on the hereditary defects of the UQCRB gene, a Turkish girl with a deletion in UQCRB and an isolated complex III defect showed hypoglycemia and lactic acidosis during a metabolic crisis in her babyhood, but had normal growth in her childhood [12]. Based on this case report, we generated the UQCRB mutant stable cell lines MT1 and MT2 and investigated their biological functions in angiogenesis. Notably, MT1 and MT2 showed remarkably increased growth and pro-angiogenic activities, together with mitochondrial structural abnormalities. Conversely, cell proliferation of UQCRB mutants was significantly decreased by treatment with the UQCRB inhibitors terpestacin and A1938.

* Corresponding author at: Chemical Genomics National Research Laboratory, Department of Biotechnology, Translational Research Center for Protein Function Control, College of Life Science & Biotechnology, Yonsei University, Seoul 120-749, Republic of Korea. Fax: +82 2 362 7265.
E-mail address: kwonhj@yonsei.ac.kr (H.J. Kwon).

http://dx.doi.org/10.1016/j.bbrc.2014.11.005
0006-291X/

In summary, these results demonstrate that UQCRB and its mutations play a key role in angiogenesis and that UQCRB mutants could be useful tools for exploring the functions of UQCRB in human cells.

2. Materials and methods

2.1. Molecular cloning

A full-length human UQCRB mutant expression vector was constructed by cloning a Polymerase Chain Reaction (PCR)-amplified full-length cDNA fragment of the UQCRB mutant (forward primer: 5′-ATGTGAATTCATGGCTGGTAAGCAGGC-3′ and reverse primer: 5′-CTCGAGGCCGTCCTCGTAGCAGCTGCAGCCGCACACCTCCAC-CACGTGGTTGCTGCGCTGGCCGTTCTTTTCTTTTCTTTCCCGAAT-3′) into the EcoRI/XhoI site of pcDNA3.1/myc-His (Invitrogen, Grand Island, NY). PCR was performed under the following conditions: initial denaturation for 5 min at 94 °C, followed by 30 cycles of 1 min at 94 °C, 1 min at 60 °C, and 1 min at 72 °C.

2.2. Generation of UQCRB mutant stable cell lines and cell culture

HEK293 cells were transfected with 1 μg UQCRB mutant expression vector by using the Lipofectamine™ LTX transfection reagent (Invitrogen, Grand Island, NY), according to the manufacturer's instructions. To select mutant colonies, 1 mg/mL of G418 (Sigma–Aldrich, Saint Louis, MO) was applied for 2 weeks, and single-cell colonies were isolated using glass cylinders (Sigma–Aldrich, Saint Louis, MO). Control (HEK293) and mutant stable cell lines were grown in Dulbecco's modified Eagle's medium (DMEM; Invitrogen, Grand Island, NY), supplemented with 10% fetal bovine serum (FBS; Invitrogen, Grand Island, NY) and 1% antibiotics (Invitrogen, Grand Island, NY). To maintain the mutant stable cell lines, 1 mg/mL G418 was applied steadily. All cells were incubated in a humidified incubator at 37 °C, with a 5% CO_2 level.

2.3. Transmission electron microscopy

Cells were harvested, washed once with PBS, and fixed with 2% paraformaldehyde/2% glutaraldehyde/0.5% $CaCl_2$ for 6 h. After washing with 0.1 M phosphate buffer, followed by 1% OsO_4 fixation, cells were dehydrated in 95% alcohol, incubated in propylene oxide for 10 min, keptin a 1:1 solution of EPON mixture and propylene oxide overnight, and embedded. Ultrathin sections were prepared with an LKB 8800 Ultratome III and were analyzed using a JEM-1011 JEOL transmission electron microscope.

2.4. Measurement of mROS levels

mROS levels were assessed by the red fluorescence mitochondrial superoxide indicator MitoSOX™ (Invitrogen, Grand Island, NY). Cells were incubated with MitoSOX (5 μM) and Hoechst 33342 (Life Technologies, Grand Island, NY) for 10 min, washed once with phosphate buffered saline (PBS), and fixed with 4% formaldehyde. Results of MitoSOX™ and Hoechst staining were analyzed under a confocal microscope (Zeiss LSM 710; Carl Zeiss MicroImaging, Thornwood, NY), and the fluorescence intensity of MitoSOX™ was measured by ImageJ.

2.5. Determination of ATP levels

Cells were distributed into white 96-well plates and incubated for 24–72 h. ATP levels were determined using ATPlite™ (Perkin Elmer, Waltham, MA), according to the manufacturer's instructions.

2.6. Cell proliferation assay

Control and mutant stable cell lines were seeded onto 96-well plates and incubated for 24–72 h. Proliferation of the cells was measured using a 3-(4,5-dimethylthiazol-2-yl)-2,5-diphenyltetrazolium bromide (MTT; Sigma–Aldrich, Saint Louis, MO) colorimetric assay.

2.7. Measurement of oxygen consumption rate

Cellular oxygen consumption rate (OCR) was measured by XF24 analyzer (Seahorse Bioscience, Billerica, MA) as previously described [13]. Briefly, 2×10^4 cells were seeded in the XF24 cell culture plates (Seahorse Bioscience, Billerica, MA). After 16 h, the medium was exchanged for 500 μL of XF Assay Medium-modified DMEM (Seahorse Bioscience, Billerica, MA) and then incubated at 37 °C without CO_2 for 1 h. OCR was measured using XF24 analyzer, and the XF24 software normalized the values to the cell number in each well. Cell number for each well was counted using a Luna™ automated cell counter (Logos, Annandale, VA).

2.8. Measurement of lactic acid production

Cells were plated onto 100Ø dishes and homogenized. After deproteinization with 10 kDa spin column, cellular lactic acid production was measured using a colorimetric assay kit (Abcam, Cambridge, MA) according to the manufacturer's instructions.

2.9. RNA isolation and reverse transcription-PCR (RT-PCR)

Total RNA was isolated using TRIzol (Invitrogen, Grand Island, NY)-based methods. RT-PCR analysis was performed to validate the expression level of each mRNA by using specific primers (wild-type UQCRB, forward: 5′-ATGTGAATTCATGGCTGGTAAG-CAGGCC-3′, reverse: 5′-ATGCCTCGAGCTTCTTTGCCCATTCTTC-3′; HIF-1a, forward: 5′-GCTGGC CCCAGCCGCTGGAG-3′, reverse: 5′-GAGTGCAGGGTCAGCACTAC-3′; VEGF, forward: 5′-ACCCATG-GCAGAAGGAGGAG-3′, reverse: 5′-GACACCAGAGTCCGACCCGG-3′; and GAPDH, forward: 5′-AACAGCGACACCCACTCCTC-3′, reverse: 5′-GGAGGGG AGATTCAGTGTGGT-3′). The expression level of the gene was quantified with Image Lab™ software (Bio-Rad, Hercules, CA).

2.10. Western blot analysis

Cell lysates were analyzed by 8%, 10%, and 12.5% sodium dodecyl sulfate polyacrylamide gel electrophoresis (SDS–PAGE) and then transferred to polyvinylidenedifluoride membranes (Millipore, Billerica, MA) by using standard methods. Blots were incubated with the following primary antibodies at 4 °C overnight: anti-UQCRB (Sigma–Aldrich, Saint Louis, MO), anti-Myc (Medical & Biological Laboratories Corp., Nagano, Japan), anti-HIF-1α (BD Bioscience, Bedford, MA), anti-VEGF (Abcam, Cambridge, MA), anti-tubulin (Millipore, Billerica, MA), and anti-actin (Abcam, Cambridge, MA). Immunolabeling was detected with an enhanced chemiluminescence (ECL) kit (GE Healthcare, Buckinghamshire, UK), according to the manufacturer's instructions. Images were quantified with Image Lab™ software (Bio-Rad, Hercules, CA).

2.11. Human VEGF enzyme-linked immunosorbent assay

UQCRB mutant stable cell lines and control cells (25×10^4 cells) were seeded onto 6-well plates with 1 mL of medium and incubated at 37 °C for 24 h. The medium was collected, and the concentration of vascular endothelial growth factor (VEGF) protein in the

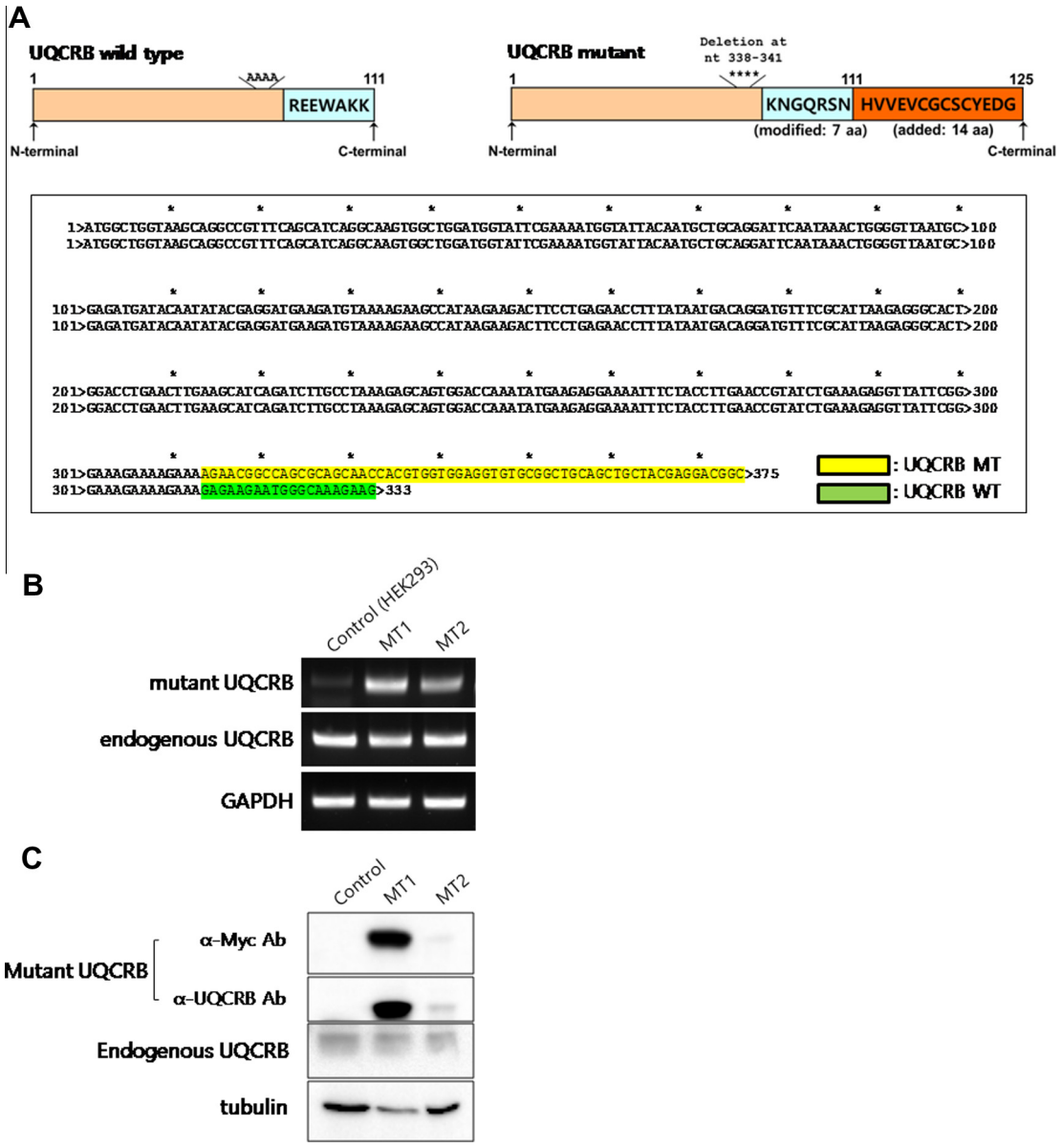

Fig. 1. Generation and validation of UQCRB mutant stable cell lines. (A) UQCRB mutant gene construct and its DNA sequence validation. (B) Expression level of mutant UQCRB and endogenous UQCRB as detected by RT-PCR. GAPDH served as an internal control. (C) Mutant stable cell lines were validated by Western blot by using anti-UQCRB and anti-Myc antibodies. Actin was used as an internal control.

supernatant was determined by a VEGF enzyme-linked immunosorbent assay (ELISA; R&D Systems, Minneapolis, MN), according to the manufacturer's instructions. The expression levels of the VEGF protein were normalized relative to that of the control samples.

2.12. In vitro invasion assay

Pro-angiogenic activity of UQCRB mutant stable cells was tested by applying the supernatants of the cells to human umbilical vascular endothelial cells (HUVECs) by using a Transwell chamber system with polycarbonate filter inserts of 8.0 μm pore size (Corning Costar, Cambridge, MA). HUVECs were grown for 7–10 passages in EBM-2 medium (Cambrex Bio Science, Baltimore, MD), supplemented with 10% FBS. The total number of invading cells was counted using a microscope (IX71; Olympus America Inc., Center Valley, PA) at 100× magnification.

2.13. Cell migration assay

Cells were seeded at a high density onto 6-well plates, and a scratch was made in the middle of the well by using a sterilized micropipette tip to create a gap of constant width. After 17 h of incubation in DMEM, the migration of cells was analyzed using a microscope.

2.14. Colony formation assay

Cells (5×10^2) were seeded onto 6-well plates and incubated for 2 weeks until colonies were formed. Cells were fixed with 4% formaldehyde, stained with 0.25% crystal violet for 10 min, and washed with double-distilled water. Stained cells were treated with 70% methanol before colorimetric measurement.

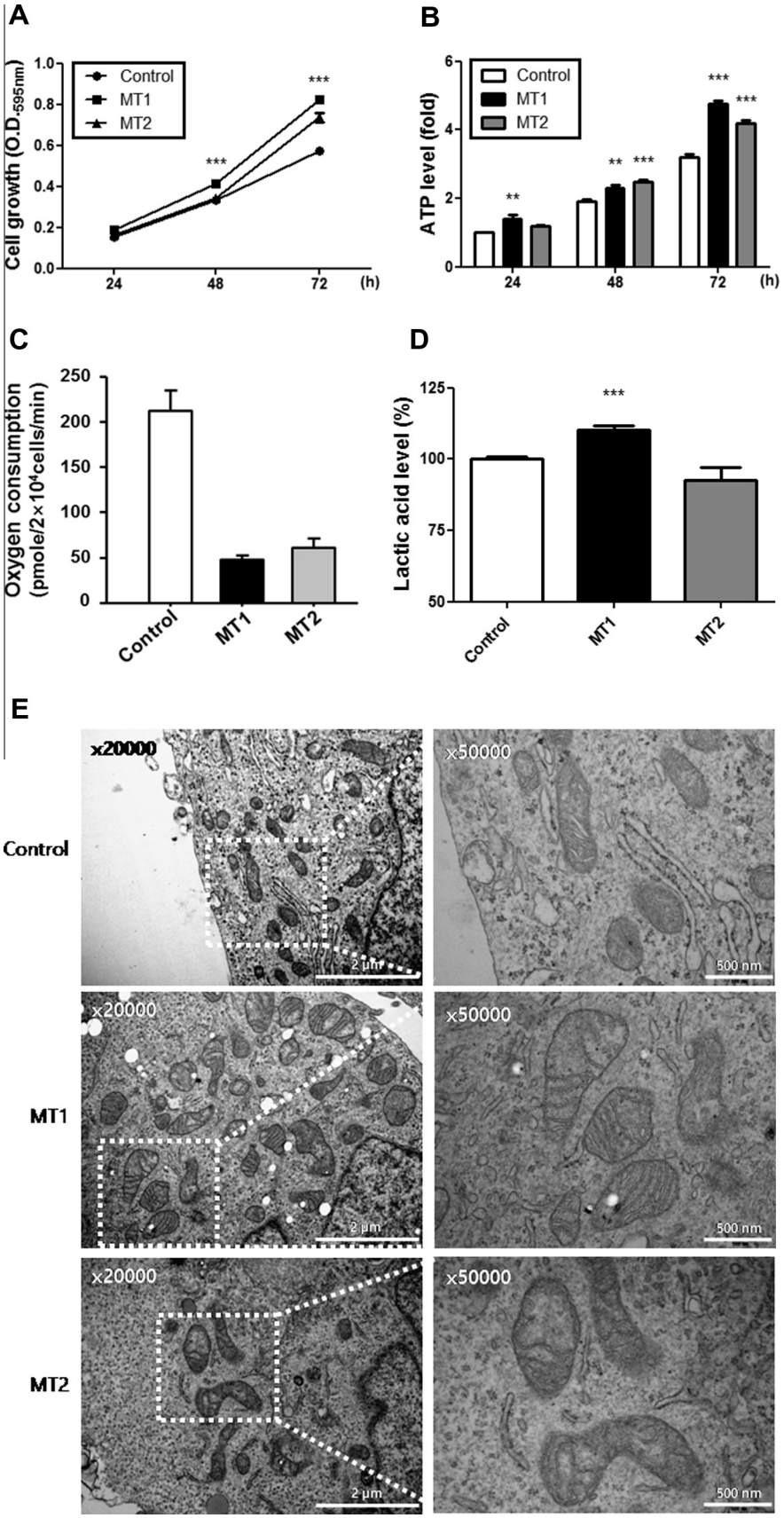

Fig. 2. Effect of UQCRB mutation on metabolic abnormality and mitochondrial morphology. (A) Proliferative activity of a UQCRB mutants determined by MTT colorimetric assay in a time-dependent manner. (B) ATP levels were quantified in a time-dependent manner. (C) Oxygen consumption of the cells. (D) Lactic acid production of the cells. Graph shows optical density units represented a mean percentage (%) of control as indicated ($p = 0.0003$). All quantified data are presented as mean ± S.E.M. compared to control ($^{**}p < 0.01$, $^{***}p < 0.001$). (E) Mitochondrial morphology of cells. Swollen mitochondria were examined compared to controls. Scale bars indicate 2000 nm and 500 nm for images of magnification 20,000× and 50,000×, respectively.

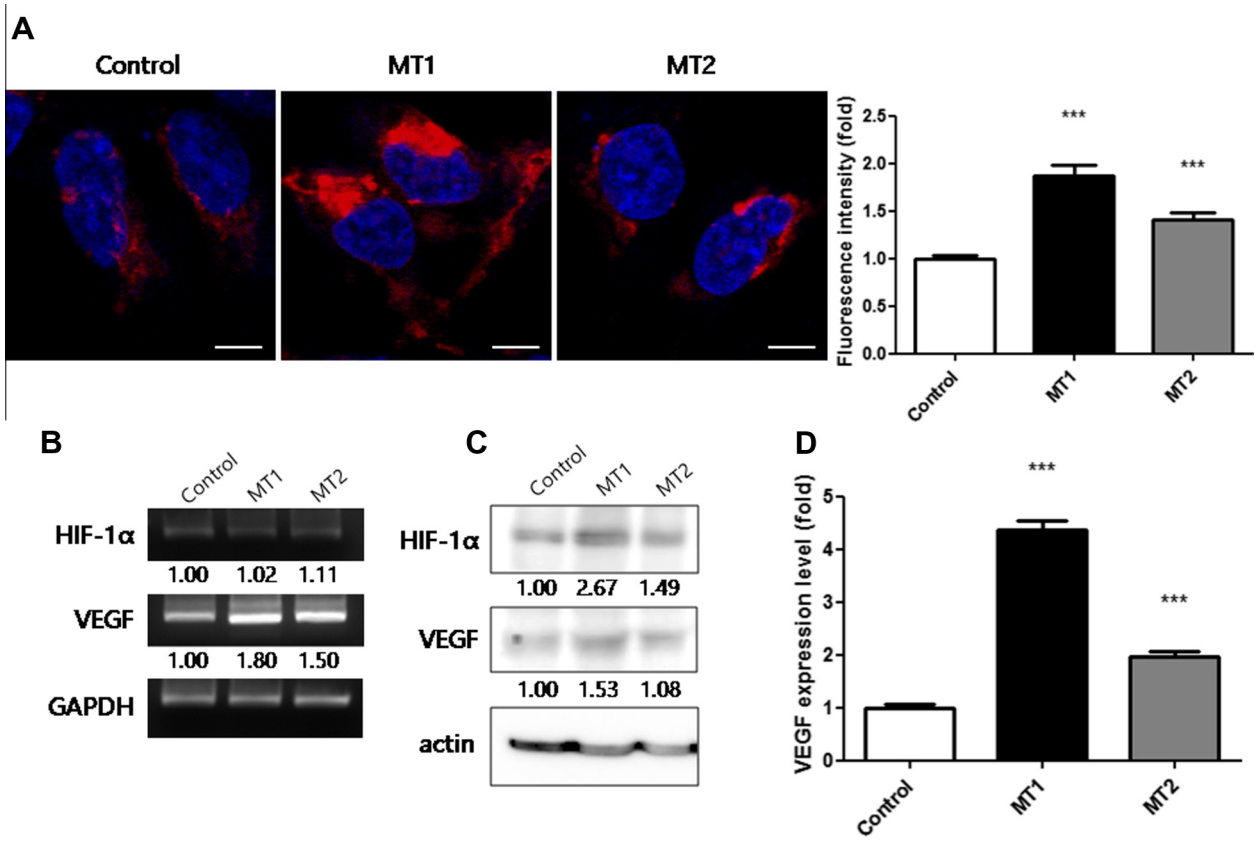

Fig. 3. Induction of VEGF expression through mROS-mediated HIF-1α expression. (A) mROS levels determined by MitoSOX™; scale bars indicate 10 μm. (B) Effect of a UQCRB mutation on HIF-1α and VEGF mRNA levels. (C) Effect of a UQCRB mutation on HIF-1α protein stabilization and VEGF protein expression. (D) Elevated level of secreted VEGF in the mutant stable cell lines. All quantified data are presented as mean ± S.E.M. compared to control ($^{***}p < 0.0001$).

2.15. Statistical analysis

Results are expressed as mean ± standard error (±S.E.M.) and all statistical analyses were calculated with GraphPad Prism (ver. 5.00 for Windows, GraphPad Software, San Diego, CA, www.graphpad.com). Student's *t*-tests were utilized to determine statistical significance between control and test groups. ANOVA (Turkey test) following bonferroni post tests was used to analyze statistical significance between three test groups. A *p*-value less than 0.05 was considered statistically significant ($^{*}p < 0.05$, $^{**}p < 0.01$, $^{***}p < 0.001$).

3. Results

3.1. UQCRB mutant stable cell lines were established based on a human case report

To investigate the biological function of UQCRB, we referred to a UQCRB mutant identified previously in human cDNA [12]. This mutant was cloned with a 4-bp deletion at nucleotides 338–341 of the UQCRB gene, based on the human case report, and subcloned for protein expression in mammalian cells. The resultant UQCRB mutant protein had alterations in seven amino acid residues and an additional stretch of 14 amino acids at the C-terminal end (Fig. 1A). The sequence of the gene construct was validated by DNA sequencing before transfection into HEK293 cells. After single-cell colony selection, two UQCRB mutant stable cell lines, comprising the same mutation but different expression levels, were named MT1 and MT2 and were analyzed at the mRNA and protein levels (Fig. 1B and C). MT1 showed a high expression level of the mutant protein, while MT2 exhibited a relatively low expression level of the mutant protein. The cell lines did not differ in their wild-type UQCRB protein expression levels.

3.2. UQCRB mutant stable cell lines exhibited proliferative activity, regardless of mitochondrial abnormalities

To characterize the UQCRB mutant stable cell lines MT1 and MT2, cell proliferation was first measured using the MTT colorimetric assay. Surprisingly, compared to controls, MT1 exhibited significantly increased growth in a time-dependent manner (Fig. 2A). The growth of MT2 was weaker than that of MT1 but stronger than that of controls. In addition, both UQCRB mutant cell lines showed increased ATP levels (Fig. 2B). Furthermore, MT1 and MT2 consumed less oxygen (Fig. 2C) and MT1 produced more lactate (Fig. 2D) than control. Notably, mitochondrial morphology of MT1 and MT2 cells showed structural abnormalities characterized by remarkable swelling (Fig. 2E).

3.3. UQCRB mutant stable cell lines induced mROS-mediated HIF1 signal transduction

Previously, Jung et al. suggested that UQCRB might play an important role in the oxygen-sensing mechanism by modulating mROS- and HIF-mediated angiogenesis under hypoxic conditions [6]. Thus, we examined mROS generation in MT1 and MT2 cells by using the mROS-specific red fluorescence indicator MitoSOX™. Notably, mROS generation was increased in both mutant cell lines compared to controls (Fig. 3A). Previous studies indicated that elevated mROS generation is essential for increased HIF-1α stability

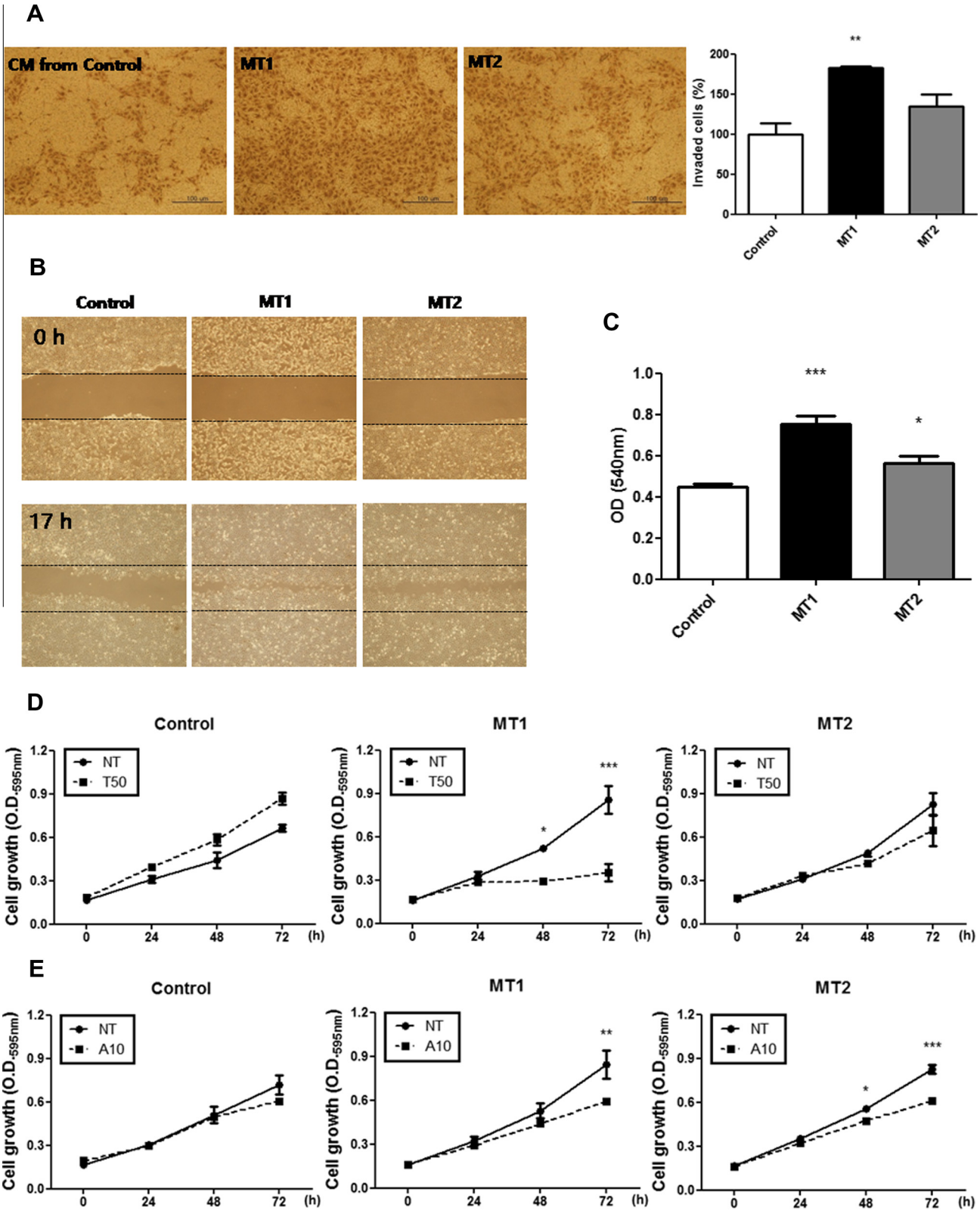

Fig. 4. Pro-angiogenic activity of UQCRB mutant stable cell lines and its regulation by UQCRB inhibitors. (A) Pro-angiogenic activity of a UQCRB mutant through conditioned media (CM)-induced invasion of HUVECs; scale bars indicate 100 μm. (B) Effect of a UQCRB mutation on cell migration; black lines indicate the edge of the gap. (C) Optical density levels of the colony formation assay by using UQCRB mutant stable cell lines or controls. (D and E) Growth of the UQCRB mutant stable cell lines regulated by the UQCRB inhibitors terpestacin (T) and A1938 (A). Cells were treated with terpestacin (50 μM) or A1938 (10 μM) in a time-dependent manner. Cell growth was measured by the MTT colorimetric assay. (F) Suppression of elevated mROS by terpestacin in UQCRB MT1 cells. mROS were measured using MitoSOX™. Terpestacin (20 μM) was applied to UQCRB MT1 cells for 1 h; scale bars indicate 20 μm. All quantified data are presented as mean ± S.E.M. compared to control ($^{*}p < 0.05$, $^{**}p < 0.01$, $^{***}p < 0.001$).

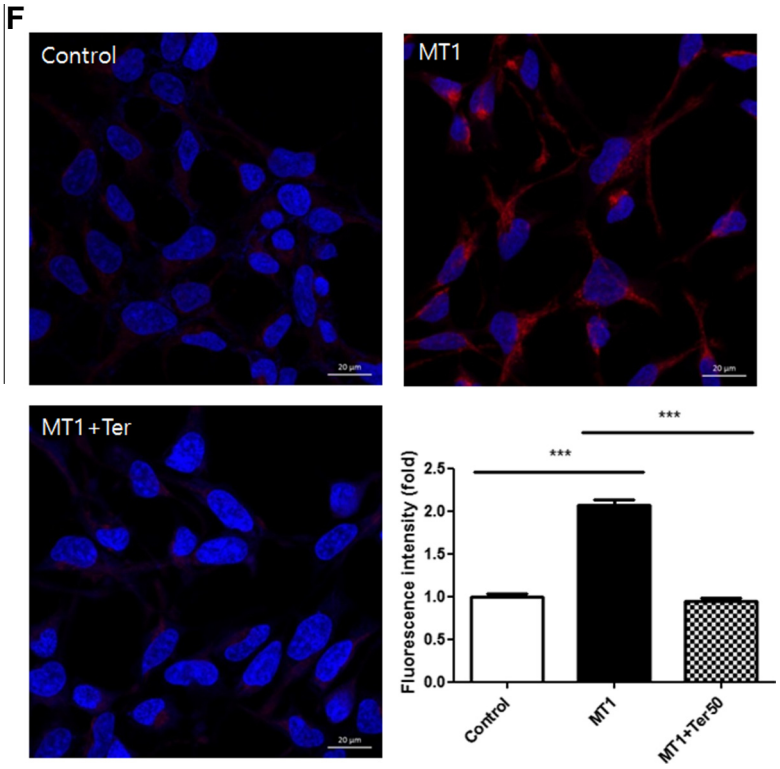

Fig. 4 (*continued*)

[14]. To test whether increased mROS generation could affect HIF-1α stability, we examined the HIF-1α protein level by Western blot. As expected, HIF-1α protein, but not mRNA, was stabilized in MT1 and MT2 cells (Fig. 3B and C). Likewise, an increased expression of the VEGF gene [15,16], downstream of HIF-1α, was observed in MT1 and MT2 cells by Western blot and RT-PCR (Fig. 3B and C). The secretion level of VEGF was measured by human VEGF ELISA. Compared to controls, MT1 showed a more than 4-fold increase of VEGF expression (Fig. 3D). These results indicated that UQCRB mutant stable cell lines significantly induced VEGF expression through mROS-mediated HIF-1α signal transduction.

3.4. The pro-angiogenic effect of UQCRB mutation is regulated by UQCRB inhibitors

Since VEGF is one of the critical cytokines in angiogenesis signaling, we confirmed the pro-angiogenic activities of MT1 and MT2 cells by various *in vitro* angiogenesis assays. First, HUVECs were treated with conditioned media, derived from MT1 and MT2, which were added to the lower chamber and incubated for 16 h. In accordance with an increased VEGF expression, the invasive activity was also significantly enhanced in HUVECs in contrast to controls (Fig. 4A). Next, cell migration of MT1 and MT2 was investigated. Compared to controls, both cell lines exhibited remarkable cell migration within 17 h (Fig. 4B). Furthermore, in the colony formation assay, MT1 and MT2 showed increased colony formation relative to that shown by controls (Fig. 4C). These data indicate that compared to controls, MT1 and MT2 have remarkably high pro-angiogenic activities.

Since UQCRB is a molecular target of the natural compound terpestacin [6], we examined the effect of terpestacin on UQCRB mutant stable cell lines. To test whether terpestacin affects MT1 and MT2, cell growth was measured with or without terpestacin for 3 days. Interestingly, terpestacin remarkably inhibited proliferation of MT1 and MT2 at a concentration of 50 μM, which did not affect the proliferation of controls (Fig. 4D). In addition, we tested the effect of A1938, a potent synthetic UQCRB inhibitor [17], on the proliferation of MT1 and MT2. As shown in Fig. 4E, compared to controls, MT1 and MT2 showed sensitivity to A1938 at a concentration of 10 μM. Notably, terpestacin treatment attenuated mROS induction in MT1 to a basal level (Fig. 4F). Overall, these results demonstrate that the proliferative and pro-angiogenic activities of MT1 and MT2 can be regulated by UQCRB inhibitors.

4. Discussion

The mitochondrion is not only an important powerhouse of the cell owing to its ability to produce majority of the ATP [18], but is also an integral member of the cell's oxygen-sensing machinery [14]. Recently, UQCRB, one of the subunits of complex III, was described as an oxygen sensor in hypoxia-induced [6] and VEGF-induced [7] angiogenesis. In addition, functional inhibition of UQCRB by gene knock-down inhibited angiogenesis in zebrafish [19]. Yet, the biological role of UQCRB is still elusive in respect with its pathological effects. Therefore, we generated UQCRB mutant stable cell lines, MT1 and MT2, based on a previous human case report through DNA overexpression in HEK293 cells. As the results, MT1 and MT2 significantly exerted biologically abnormal activities compared to control in a mutant expression-dependent manner, suggesting that UQCRB mutant functioned dominant negative effect toward complex III. It is well known that suppression of mitochondrial respiration augments ROS production [20–22]. Particularly, mitochondrial complex III, which catalyzes electron transfer from ubiquinol to cytochrome c, is a major ROS generation site through an electron gradient [20]. Together with suppressed OXPHOS owing to declined complex III activity, mitochondrial electron transport complexes might produce more ROS leading to biologically abnormal activities of MT1 and MT2 cells. Further analysis of mitochondrial complex activities in the UQCRB mutant

stable cell lines will be investigated in the following studies. As inferred from the proliferative and pro-angiogenic activities of UQCRB mutant stable cell lines, both MT1 and MT2 cells exert transformed cell activities leading to increased glycolysis rate. This is consistent with the clue of patient with UQCRB mutant, who showed hypoglycemia [12], which can be caused by increased glucose uptake. In addition, it is well characterized that HIF1 activation induces amplification of genes encoding glucose transporters and most glycolytic enzymes to enhance glycolysis [23]. Indeed, both MT1 and MT2 cells exhibited HIF-1α stabilization (Fig. 3C), implying that the rate of glycolysis could be elevated in UQCRB mutant stable cell lines. Furthermore, oxygen consumption rate (OCR) is mainly in opposite relations with glycolysis in highly proliferative cells [24,25]. Cells with a glycolytic phenotype exhibit significantly higher rates of extracellular acidification rate (ECAR), an indicator of glycolysis, than cells using oxidative phosphorylation (oxygen consumption rate; OCR). In the analysis of OCR in MT1 and MT2, we detected down-regulation of OCR in both cell lines (Fig. 2C). Furthermore, as a direct evidence of increase in glycolysis, we found that MT1 cells produced more lactic acid, a product of anaerobic glycolysis, than normal control cells (Fig. 2D). Lactic acid generation is also a similar phenotype of lactic acidosis with the patient bearing UQCRB mutant. In these respects, the UQCRB mutant stable cell lines could be characterized as glycolytic cells, resulting from a mutation in UQCRB-derived alterations to intracellular signaling pathways that affect cell metabolism and proliferative activities. Mitochondrial alteration has long been proposed to play an important role in tumorigenesis [26,27]. Baysal et al. demonstrated how mutations in the mitochondrial complex II gene SDHD could contribute to tumor formation [28]. This proposed redox stress mechanism with increased mROS generation in mitochondria, resulting in pseudo-hypoxia, would be consistent with our results, linking mitochondrial abnormality to angiogenesis-related disease and cancer [29]. Interestingly, we demonstrated that the proliferation of MT1 and MT2 could be regulated by the UQCRB inhibitors terpestacin and A1938. It is conceivable that inhibition of mROS by UQCRB inhibitors could affect cell growth.

In summary, our results propose a molecular basis for UQCRB mutant-related biological processes. In addition, this study contributes to our understanding of the link between mitochondrial abnormalities caused by mutations in UQCRB and angiogenesis- or mitochondria-related diseases. Furthermore, these results point to options for correcting the pathological effects of UQCRB mutations by UQCRB inhibitors.

Acknowledgments

This study was partly supported by Grants from the National Research Foundation of Korea funded by the Korean Government (2010-0017984, 2012M3A9D1054520), the Translational Research Center for Protein Function Control, KRF (2009-0083522), the Next-Generation BioGreen 21 Program (No. PJ0079772012), Rural Development Administration, National R&D Program, Ministry of Health &Welfare (0620360-1), and the Brain Korea 21 Plus Project, Republic of Korea.

References

[1] J. Nunnari, A. Suomalainen, Mitochondria: in sickness and in health, Cell 148 (2012) 1145–1159.
[2] D.C. Wallace, Mitochondria and cancer, Nat. Rev. Cancer 12 (2012) 685–698.
[3] P. Dromparis, E.D. Michelakis, Mitochondria in vascular health and disease, Annu. Rev. Physiol. 75 (2013) 95–126.
[4] K.F. Petersen, S. Dufour, D. Befroy, R. Garcia, G.I. Shulman, Impaired mitochondrial activity in the insulin-resistant offspring of patients with type 2 diabetes, N. Engl. J. Med. 350 (2004) 664–671.
[5] H. Suzuki, Y. Hosokawa, H. Toda, M. Nishikimi, T. Ozawa, Cloning and sequencing of a cDNA for human mitochondrial ubiquinone-binding protein of complex III, Biochem. Biophys. Res. Commun. 156 (1988) 987–994.
[6] H.J. Jung, J.S. Shim, J. Lee, Y.M. Song, K.C. Park, S.H. Choi, N.D. Kim, J.H. Yoon, P.T. Mungai, P.T. Schumacker, H.J. Kwon, Terpestacin inhibits tumor angiogenesis by targeting UQCRB of mitochondrial complex III and suppressing hypoxia-induced reactive oxygen species production and cellular oxygen sensing, J. Biol. Chem. 285 (2010) 11584–11595.
[7] H.J. Jung, Y. Kim, J. Chang, S.W. Kang, J.H. Kim, H.J. Kwon, Mitochondrial UQCRB regulates VEGFR2 signaling in endothelial cells, J. Mol. Med. (Berl.) 91 (2013) 1117–1128.
[8] H.L. Jia, Q.H. Ye, L.X. Qin, A. Budhu, M. Forgues, Y. Chen, Y.K. Liu, H.C. Sun, L. Wang, H.Z. Lu, F. Shen, Z.Y. Tang, X.W. Wang, Gene expression profiling reveals potential biomarkers of human hepatocellular carcinoma, Clin. Cancer Res. 13 (2007) 1133–1139.
[9] K.O. Wrzeszczynski, V. Varadan, J. Byrnes, E. Lum, S. Kamalakaran, D.A. Levine, N. Dimitrova, M.Q. Zhang, R. Lucito, Identification of tumor suppressors and oncogenes from genomic and epigenetic features in ovarian cancer, PLoS One 6 (2011) e28503.
[10] T. Harada, C. Chelala, T. Crnogorac-Jurcevic, N.R. Lemoine, Genome-wide analysis of pancreatic cancer using microarray-based techniques, Pancreatology 9 (2009) 13–24.
[11] J. Lascorz, M. Bevier, W.V. Schonfels, H. Kalthoff, H. Aselmann, J. Beckmann, J. Egberts, S. Buch, T. Becker, S. Schreiber, J. Hampe, K. Hemminki, A. Forsti, C. Schafmayer, Polymorphisms in the mitochondrial oxidative phosphorylation chain genes as prognostic markers for colorectal cancer, BMC Med. Genet. 13 (2012) 31.
[12] S. Haut, M. Brivet, G. Touati, P. Rustin, S. Lebon, A. Garcia-Cazorla, J.M. Saudubray, A. Boutron, A. Legrand, A. Slama, A deletion in the human QP-C gene causes a complex III deficiency resulting in hypoglycaemia and lactic acidosis, Hum. Genet. 113 (2003) 118–122.
[13] S.H. Jeong, I.S. Song, H.K. Kim, S.R. Lee, S. Song, H. Suh, Y.G. Yoon, Y.H. Yoo, N. Kim, B.D. Rhee, K.S. Ko, J. Han, An analogue of resveratrol HS-1793 exhibits anticancer activity against MCF-7 cells via inhibition of mitochondrial biogenesis gene expression, Mol. Cells 34 (2012) 357–365.
[14] T. Klimova, N.S. Chandel, Mitochondrial complex III regulates hypoxic activation of HIF, Cell Death Differ. 15 (2008) 660–666.
[15] D.E. Richard, E. Berra, J. Pouyssegur, Angiogenesis: how a tumor adapts to hypoxia, Biochem. Biophys. Res. Commun. 266 (1999) 718–722.
[16] J.A. Forsythe, B.H. Jiang, N.V. Iyer, F. Agani, S.W. Leung, R.D. Koos, G.L. Semenza, Activation of vascular endothelial growth factor gene transcription by hypoxia-inducible factor 1, Mol. Cell. Biol. 16 (1996) 4604–4613.
[17] H.J. Jung, K.H. Kim, N.D. Kim, G. Han, H.J. Kwon, Identification of a novel small molecule targeting UQCRB of mitochondrial complex III and its anti-angiogenic activity, Bioorg. Med. Chem. Lett. 21 (2011) 1052–1056.
[18] C. Desler, L.J. Rasmussen, Mitochondria in biology and medicine – 2012, Mitochondrion 16 (2014) 2–6.
[19] Y.S. Cho, H.J. Jung, S.H. Seok, A.Y. Payumo, J.K. Chen, H.J. Kwon, Functional inhibition of UQCRB suppresses angiogenesis in zebrafish, Biochem. Biophys. Res. Commun. 433 (2013) 396–400.
[20] J.F. Turrens, Mitochondrial formation of reactive oxygen species, J. Physiol. 552 (2003) 335–344.
[21] M.L. Taddei, E. Giannoni, G. Raugei, S. Scacco, A.M. Sardanelli, S. Papa, P. Chiarugi, Mitochondrial oxidative stress due to complex I dysfunction promotes fibroblast activation and melanoma cell invasiveness, J. Signal Transduct. 2012 (2012) 684592.
[22] S. Drose, U. Brandt, The mechanism of mitochondrial superoxide production by the cytochrome bc1 complex, J. Biol. Chem. 283 (2008) 21649–21654.
[23] X. Wang, S. Peralta, C.T. Moraes, Mitochondrial alterations during carcinogenesis: a review of metabolic transformation and targets for anticancer treatments, Adv. Cancer Res. 119 (2013) 127–160.
[24] M. Wu, A. Neilson, A.L. Swift, R. Moran, J. Tamagnine, D. Parslow, S. Armistead, K. Lemire, J. Orrell, J. Teich, S. Chomicz, D.A. Ferrick, Multiparameter metabolic analysis reveals a close link between attenuated mitochondrial bioenergetic function and enhanced glycolysis dependency in human tumor cells, Am. J. Physiol. Cell Physiol. 292 (2007) C125–136.
[25] H.R. Christofk, M.G. Vander Heiden, M.H. Harris, A. Ramanathan, R.E. Gerszten, R. Wei, M.D. Fleming, S.L. Schreiber, L.C. Cantley, The M2 splice isoform of pyruvate kinase is important for cancer metabolism and tumour growth, Nature 452 (2008) 230–233.
[26] J.S. Park, L.K. Sharma, H. Li, R. Xiang, D. Holstein, J. Wu, J. Lechleiter, S.L. Naylor, J.J. Deng, J. Lu, Y. Bai, A heteroplasmic, not homoplasmic, mitochondrial DNA mutation promotes tumorigenesis via alteration in reactive oxygen species generation and apoptosis, Hum. Mol. Genet. 18 (2009) 1578–1589.
[27] S. Ohsawa, Y. Sato, M. Enomoto, M. Nakamura, A. Betsumiya, T. Igaki, Mitochondrial defect drives non-autonomous tumour progression through Hippo signalling in Drosophila, Nature 490 (2012) 547–551.
[28] B.E. Baysal, R.E. Ferrell, J.E. Willett-Brozick, E.C. Lawrence, D. Myssiorek, A. Bosch, A. van der Mey, P.E. Taschner, W.S. Rubinstein, E.N. Myers, C.W. Richard 3rd, C.J. Cornelisse, P. Devilee, B. Devlin, Mutations in SDHD, a mitochondrial complex II gene, in hereditary paraganglioma, Science 287 (2000) 848–851.
[29] E. Gottlieb, I.P. Tomlinson, Mitochondrial tumour suppressors: a genetic and biochemical update, Nat. Rev. Cancer 5 (2005) 857–866.